Manuscript submitted to:
Sensors and Actuators, B: Chemical

IN-LINE CAPACITANCE SENSOR FOR REAL-TIME WATER ABSORPTION MEASUREMENTS

Mark A. Nurge[a] and Stephen A. Perusich[b,*]

[a] - *John F. Kennedy Space Center, NASA, Applied Physics Laboratory, Mail Code: NE-L5, Kennedy Space Center, Florida 32899 USA; E-Mail: Mark.A.Nurge@nasa.gov.*

[b] - *John F. Kennedy Space Center, ASRC Aerospace Corporation, Applied Science and Technology, Mail Code: ASRC-24, Kennedy Space Center, Florida 32899 USA; E-Mail: Stephen.A.Perusich@nasa.gov.*

[*] - *Author to whom correspondence should be addressed (Phone: 321-861-2945, Fax: 321-867-2317).*

March, 2010

Abstract

A capacitance/dielectric sensor was designed, constructed, and used to measure in real time the *in-situ* water concentration in a desiccant water bed. Measurements were carried out with two experimental setups: (1) passing nitrogen through a humidity generator and allowing the gas stream to become saturated at a measured temperature and pressure, and (2) injecting water via a syringe pump into a nitrogen stream. Both water vapor generating devices were attached to a downstream vertically-mounted water capture bed filled with 19.5 g of Moisture Gone™ desiccant. The sensor consisted of two electrodes: (1) a 1/8" dia stainless steel rod placed in the middle of the bed and (2) the outer shell of the stainless steel bed concentric with the rod. All phases of the water capture process (background, heating, absorption, desorption, and cooling) were monitored with capacitance. The measured capacitance was found to vary linearly with the water content in the bed at frequencies above 100 kHz indicating dipolar motion dominated the signal; below this frequency, ionic motion caused nonlinearities in the water concentration/capacitance relationship. The desiccant exhibited a dielectric relaxation whose activation energy was lowered upon addition of water indicating either a less hindered rotational motion or crystal reorientation.

Keywords: capacitance, sensor, water, absorbent, desiccant, dielectric constant

1. Background and Theory

Capacitance or dielectric measurements are based on applying an alternating electric field across a material and examining the orientation of permanent and induced dipoles and the separation of positive and negative ions in the material. The motion of dipoles and ions can be represented by a complex admittance (Y in Ω^{-1}) defined as

$$Y = \frac{I}{V} = \frac{I_{in} + iI_{out}}{V} = \frac{I_o \sin\delta + iI_o \cos\delta}{V} \tag{1}$$

where, I is the total current (Amps), V is the voltage (Volts), I_{in} is the in-phase current with the voltage (Amps), I_{out} is the out-of-phase current with the voltage (Amps), I_o is the amplitude of the total current (Amps), and δ is the phase angle (degrees) [1].

The complex capacitance (C^* in Farads) is composed of a real capacitance (C in Farads) and an imaginary capacitance or dissipation (D in Farads) and related to the real and imaginary components of the complex permittivity by the capacitance in a vacuum (C_o in Farads).

$$C^* = C + iD = C_o\varepsilon^* = C_o(\varepsilon' + i\varepsilon'') \tag{2}$$

Knowledge of the sensor geometry allows the computation of the absolute dielectric permittivity (ε') and the dielectric loss factor (ε'') and, therefore, the complex permittivity (ε^*). The dielectric permittivity is a measure of the dipole concentration as well as the motion and/or orientation of dipoles and ions in an AC field whereas the loss factor represents the energy expended during dipole or ion movement. For a parallel plate geometry, the computation of ε' and ε'' is trivial for a homogeneous material; however, for a more complex geometry or highly inhomogeneous materials, the computation can be much more involved. The temperature and applied frequency also affect the measured C and ε'. If all other variables are constant, C and ε' may either increase or decrease with temperature; ε' generally decreases with temperature for gases but increases and then decreases

with temperature for solids. In general, C and ε' decrease with frequency; at extremely high frequencies, C and ε' are generally independent of frequency.

When a voltage is applied across a material, the electrical energy is absorbed by dipoles and ions in the material resulting in degrees of polarization and various atomic and molecular relaxations. A relaxation is the movement of a dipole and/or ion to its lowest energy state (lowest impedance); the relaxation time is the elapsed time taken to achieve this relaxed state. At low frequencies or high temperatures, the dipole/ion has sufficient time or enough thermal energy to fully relax, but at high frequencies or low temperatures the dipole/ion either cannot keep up with the applied high frequency field or does not have enough thermal energy so that the dipole/ion never attains a fully relaxed state but may attain a steady unrelaxed ("frozen") state.

The relationship between composition and either capacitance or dielectric permittivity is given below. The dielectric properties of a material placed between two capacitor electrodes is

$$\varepsilon' = \frac{Q + P}{Q} = \frac{C}{C_o} \tag{3}$$

where, Q is the charge per unit area on the capacitors in a vacuum (Coulombs/m^2) and P is the additional charge per unit area on the capacitors with a material present (Coulombs/m^2). The value of Q is a constant for a given system, but P varies with the concentration or type of material present. The method of obtaining P (typically called the polarization when written as a vector) is to relate it to concentration by summing the dipolar and ionic components using the following equation [2]

$$P = n_d N_A \mu_d + n_i N_A \mu_i \tag{4}$$

where, n_d is the concentration of dipoles per unit volume (moles of dipoles/m^3), N_A is Avogadro's number (6.023×10^{23} dipoles/mol), μ_d is the dipole moment of the material (C-m), n_i is the concentration of ions present per unit volume (moles of ions/m^3), and μ_i is the dipole moment of an

ion-ion pair (C-m). Equations (3) and (4) show the relationship between the dielectric permittivity and the concentration, but the dipole moments are not always straightforward to evaluate.

The dipole moment for the ion-ion pair is simply expressed as

$$\mu_i = q_e \ell_i \tag{5}$$

where, q_e is the elemental charge ($1.6\text{x}10^{-19}$ C), and ℓ_i is the distance between ions (m).

The dipole moment for the covalently bonded dipoles requires a more rigorous calculation, such as using the Fröhlich modification of Onsager's equation [3]

$$\mu_d^2 = \frac{3kT}{4\pi n_d g}\left(\varepsilon_r - \varepsilon_u\right)\left(\frac{2\varepsilon_r + \varepsilon_u}{3\varepsilon_r}\right)\left(\frac{3}{\varepsilon_u + 2}\right)^2 \tag{6}$$

where, k is Boltzmann's constant (1.381×10^{-23} J/K), T is absolute temperature (K), g is the Kirkwood factor [3], ε_r is the relaxed permittivity, and ε_u is the unrelaxed permittivity.

Therefore, substituting Equation (4) into Equation (3) gives a direct relationship between the concentration and dielectric variables.

$$\varepsilon' = \frac{Q + N_A(n_d\mu_d + n_i\mu_i)}{Q} = \frac{C}{C_o} \tag{7}$$

Equation (7) shows that the dielectric variables (ε' and C) are directly proportional to the dipole concentration (water content). This theoretical relationship was tested experimentally in the present work where the water content in the absorption bed was found to be directly proportional to the measured capacitance, as predicted by Equation (7).

The literature revealed several papers on capacitance measurements in packed beds mainly used to measure void fraction and flow profiles [5 - 7]. This technique is in recent years referred to

as Electrical Capacitance Tomography (ECT). No mention of *in-situ* capacitance measurements of water concentration in packed beds has been found.

2. Experimental Methods

The capacitance probe consisted of two electrodes. The first electrode was a 1/8" diameter stainless steel rod inserted down the middle of the water bed. On one end, the rod was seated in a ceramic flange. The other end was fitted with a sleeve and protruded out the end of the bed. The second electrode was the outer casing of the water bed. Therefore, the field lines ran radially between the center rod and the bed casing. The water bed used in all experiments is shown without the sensor in Figure 1. The absorbent used in the water bed was Moisture Gone (Haitt Distributors, Ltd) consisting of an alumina silicate zeolite structure. X-ray Photoelectron Spectroscopy (XPS) elucidated the chemical composition of the absorbent [4].

This geometry forms a cylindrical capacitor of length L, with inner conductor of radius r_1 and an outer conductor with inner radius r_2. The equation for capacitance is then given by

$$C = \frac{2\pi\varepsilon_o}{\ln(r_2/r_1)}\varepsilon' L \tag{8}$$

where, ε_o is the permittivity of free space and ε' is the relative dielectric constant of the material between the conductors. In this case, the dielectric material between the conductors is a desiccant that is either totally dry, totally wet, or some state in between the two extremes. If it is assumed that the moisture flows into one end of the sensor and evenly fills each cross-sectional disk of desiccant with moisture, a linear expression can be derived for the capacitance as a function of the axial position of the wet/dry interfacial layer (z):

$$C(z) = \frac{2\pi\varepsilon_o}{\ln(r_2/r_1)}\left[\left(\varepsilon_w' - \varepsilon_d'\right)z + \varepsilon_d' L\right] \tag{9}$$

where ε_w' is the relative dielectric constant of the totally wet desiccant and ε_d' is the relative dielectric constant of the totally dry desiccant. The interface layer will not be flat since the velocities near the conductor walls approach zero. However, the long thin geometry will minimize the errors due to this effect, still allowing the expectation of a linear response from the sensor as a function of moisture content. In addition, the desiccant particles act as a static mixer thereby leveling out the velocity distribution.

Two experimental setups were used to evaluate the capacitance sensor. The first setup, shown in Figure 2, used an in-house made humidity chamber to generate a constant humidity or water concentration in the feed line to the water bed. Nitrogen was used as the inert carrier gas. The appeal of this setup was the ability to go to high flow rates (up to 5 l/min). The inlet water concentrations to the bed were dependent on accurate temperature and pressure measurements within the humidity chamber. This experimental setup required disconnecting and weighing the water bed after each absorption to measure the amount of water absorbed by the desiccant. The electrical leads were sent to an LCR meter (HP 4284A) interfaced to a PC. Ten frequencies from 10 kHz to 1 MHz were taken at 1 second intervals and then the system was allowed to rest for 1 second so a measurement cycle was 11 seconds long.

The second setup used a syringe pump to meter into the line a known quantity of water vapor which was swept away by a nitrogen stream, as shown in Figure 3. Again, the carrier gas was nitrogen. This setup differs from the first setup in a number of ways. A syringe pump replaces the humidity chamber. In addition, to electrically isolate the sensor from the rest of the equipment, Teflon® tube spacers were added to the lines at the top and bottom of the water bed. The rate and volume of the liquid water displaced by the syringe pump was checked and found to be accurate. However, towards the end of the syringe tip, as the water vaporizes and expands into the flow stream, the vapor fluid dynamics are not fully defined.

Each system was heat wrapped with high temperature heating tape (Omega). To insure that the N_2 inlet gas was sufficiently heated, a coiled section of tubing was added which allowed preheating of the inlet nitrogen gas stream.

3. ***Discussion of Results***

To test the consistency of the capacitance signal, the bed was dried overnight at 230°C with a N_2 purge. The bed was sealed and held at 130°C overnight. The results are shown in Figure 4. For the first hour, the bed was still cooling, but for the remainder of the time, the bed was maintained fairly constant at 130°C. The origins of the data oscillations are unknown but could be due to either electronic noise or oscillations of the double layers at the electrode surface. At high frequencies, the oscillations diminished resulting in a more stable capacitance signal. It is interesting to note that closely examining even the highest frequency curve yields a slightly decreasing trend. This trend is most likely caused by either a drift in the electronics or the water slowly desorbing from the desiccant.

In Figure 5, the humidity chamber was used to produce a gas stream of 700 ml/min into a water bed held at 130°C. After the first 5 minutes (background reading), the steady influx of water into the bed is shown as a linear response of the capacitance signal at 1 MHz. At 56 minutes, the relative humidity measured at the water bed exit increased dramatically indicating the water bed was nearing it's capacity (breakthrough). The capacitance did not actually plateau until about 90 minutes when the RH was close to 100%. Past 105 minutes, the bed was cooled at a constant water content thus lowering the capacitance.

A water step experiment was conducted to see if plateaus could be measured at discrete water concentrations. The syringe pump apparatus alternately metered in 0.5 g water over 5 minutes, then stopped the water flow (still leaving the nitrogen flowing), and repeated this procedure

4 times. The results, shown in Figure 6, illustrate the steps. At low water concentrations in the bed, the plateau is very distinct while at higher water concentrations the data take longer to stabilize. Perhaps at low concentrations, the water quickly finds a site for absorption. At higher concentrations, diffusion of the gas must occur in order to find an appropriate site to absorb. In addition, the temperature was very difficult to stabilize probably because of the heat of absorption so the plateaus are influenced by these temperature transients.

The mean plateau values from Figure 6 were obtained and plotted in Figure 7. Also plotted are the low and high values of the "plateau" which are represented as the error bars. A linear relationship exists between the water introduced to the bed and the measured capacitance.

Desorption was also examined with the present capacitance technique. Desorption requires raising the bed temperature from 130 to 230°C for a period of time to dehydrate the absorbent. A N_2 purge (used here) and/or vacuum can be used to suck the water from the bed at the elevated temperature. The process is measured in Figure 8 for a bed containing 2.28 g of absorbed water using the humidity chamber apparatus. Over the first 28.5 minutes, the bed temperature was ramped up to 230°C; then the temperature was maintained at 230°C overnight taking capacitance readings over 10 frequencies every 11 seconds (three frequency curves are omitted from Figure 8 for clarity).

During the initial heat-up period, the capacitance of the desiccant tends to increase due to the increased temperature but decrease since the bed is losing water. In addition, water may migrate from the hotter outer electrode towards the cooler center electrode. After 28.5 minutes, the temperature is maintained at 230°C so the decreasing capacitance behavior is entirely due to the decreasing water concentration in the bed. Note that over the first 100 or so minutes, the bulk of the water is desorbed; however, despite desorbing for more than 16 hours, the capacitance still did not plateau indicating extremely slow mass transfer processes occurring at the low water concentrations. Cooling curves were also recorded, as shown in Figure 9.

Calculation of the dissipation factor (dissipation divided by capacitance) over the range of operating temperatures and frequencies revealed a series of relaxation peaks, as shown in Figure 10. A classic activation model is assumed in the form of

$$f = f_o e^{-\frac{E}{RT}} \tag{10}$$

where, f = frequency (Hz), f_o = pre-exponential constant (Hz), E = activation energy (cal/mol), and R = universal gas constant (1.987 cal/mol-K). Taking the log of both sides reveals a typical Arrhenius linear relationship between $\log f$ and $1/T$. The temperature (T in K) referred to in equation (10) is the peak temperature of a constant frequency curve (relaxation) found in Figure 10.

The Arrhenius plot is shown in Figure 11. An activation energy of 14.15 kcal/mol is computed from the slope of the line in Figure 11 indicative of a localized motion within the absorbent. A separate experiment was conducted with a saturated water bed. The peaks were not as dominate and were shifted to lower temperatures and dissipation factor values. The activation energy for the system containing water was 6.41 kcal/mol possibly indicating that the presence of water aids in the absorbent relaxation.

Using the syringe pump at 130°C with flow rates of 0.1 ml H_2O/min and 250 ml N_2/min, the capacitance curves in Figure 12 were determined. These are calibration curves for the system; thus by measuring a capacitance at a known frequency, the water content in the bed can be determined from the graph. The curves at high frequency show linearity indicating dipolar motions while the nonlinearities at lower frequencies indicate the additional capacitance due to ionic motions.

An experiment was conducted to determine how fast the entire process would take. The water flow rate was doubled to 0.2 ml/min from the experiment in Figure 12. Figure 13 shows measurements for the entire process. From 0 to 5 minutes, a background signal was measured. From 5 to 15 minutes, water flowed into the bed; a linear capacitance response was observed (as

shown by the expanded portion depicted in Figure 14). From 15 to 78 minutes, the water flow was shut off, and the bed was heated and maintained at 230°C; the desorption is measured with decreasing capacitance. After 78 minutes, the controllers were shut off and the system was allowed to cool down; the capacitance decreased due to temperature.

4. Conclusions

The measured capacitance from the cylindrical sensor was shown both theoretically and experimentally to be directly proportional to the water introduced to the desiccant bed. A linear relationship exists at high frequencies emanating from dipolar relaxations while nonlinearities occur at lower frequencies due to ionic effects. This water measurement technique was successfully incorporated into an In-Situ Resource Utilization (ISRU) NASA/ASRC process designed to separate and capture water for future lunar missions.

Acknowledgments

The authors wish to thank Dr. Steve Trigwell for using his XPS expertise to uncover critical information concerning the desiccant composition. In addition, thanks to many NASA and ASRC Aerospace personnel involved with the Regolith and Environment Science and Oxygen and Lunar Volatile Extraction (RESOLVE) project for their insightful comments throughout this project. Financial support was graciously provided by the KSC NASA ISRU program.

References

1. S. Perusich, M. McBrearty, Dielectric Spectroscopy for Polymer Melt Composition Measurements, Poly. Eng. Sci. 40 (2000) 214-226.
2. A. R. Blythe, Electrical Properties of Polymers, Cambridge University Press, Cambridge, England, 1979.
3. H. Fröhlich, Theory of Dielectrics, second ed., Oxford, England, 1958.
4. S. Trigwell, K-Alpha Sample Analysis Report, Memo to S. Perusich, Kennedy Space Center, 2008.
5. S. M. Huang, A. Plaskowski, C. G. Xie, M. S. Beck, Capacitance-Based Tomographic Flow Imaging System, Electronics Letters 24 (1988) 418-419.
6. A. J. Jaworski, G. T. Bolton, The Design of an Electrical Capacitance Tomography Sensor for Use with Media of High Dielectric Permittivity, Meas. Sci. Tech. 11 (2000) 743-757.
7. S. Liu, Q. Chen, H. G. Wang, F. Jiang, I. Ismail, W. Q. Yang, Electrical Capacitance Tomography for Gas–Solids Flow Measurement for Circulating Fluidized Beds, Flow Meas. Instrumentation 16 (2005) 135-144.

Vitae

Mark A. Nurge, Ph.D., P.E.

Mark has received degrees in electrical engineering (Bachelor's and M.S.) from Georgia Institute of Technology. Later, he earned an M. S. in Engineering Management as well as M.S. and Ph.D. degrees in physics from the University of Central Florida. Mark has worked for NASA at Kennedy Space Center (KSC) for 23+ years in a variety of engineering and management positions involving electronic sensors and instrumentation. Presently, he is responsible for conducting research and development on capacitance and inductance based sensing technologies for application to the Space Shuttle, Payloads, Expendable Launch Vehicles, and future vehicles.

Stephen A. Perusich, Ph.D.

Steve received degrees in chemical engineering from Lehigh University (B.S.) and the University of Illinois at Urbana-Champaign (M.S. and Ph.D.). After graduation, he performed research at E. I. DuPont de Nemours' Experimental Station in the areas of polymer physics, advanced materials, and sensors. Steve then joined the faculty at Auburn University where he taught undergraduate and graduate courses in chemical engineering as well as performed research in neurochemical engineering, nonaqueous ionomer transport, and mathematical modeling. Steve then accepted a position at the Kennedy Space Center where he has participated in the In-Situ Resource Utilization, applied chemistry, and planetary particle physics programs.

Figure Captions

1. (a) Water desiccant bed without sensor; (b) end-view of bed with sensor
2. Humidity chamber experimental setup
3. Syringe pump experimental setup
4. Sealed dry water bed maintained at 130°C overnight
5. Capacitance, temperature, and relative humidity measurements using the humidity chamber setup; temperature (T_{bed}) refers to the right hand axis; all other plots refer to the left hand axis
6. Stepped water experiment using 0.5 g H_2O increments and the syringe pump setup; N_2 flow rate = 250 ml/min; H_2O flow rate = 0.1 ml/min; f = 1 MHz; T = 130°C
7. Plateau capacitance values; error bars indicate the extremes in the capacitance at a given step; syringe pump setup; N_2 flow rate = 250 ml/min; H_2O flow rate = 0.1 ml/min; f = 1 MHz; T = 130°C; regression: $C = 27.87\,[H_2O] + 22.192$; $r^2 = 0.995$
8. Desorption at 230°C overnight
9. Cooling a dry water bed; data points were fit by 4 parameter sigmoidal regressions
10. Dissipation factor peaks during cooling after desorption of a dry water bed
11. Arrhenius plot of the dry Moisture Gone during cooling after desorption; E_a = 14.15 kcal/mol, r^2 = 0.9904
12. Water/capacitance calibration using the syringe pump setup; N_2 flow rate = 250 ml/min; H_2O flow rate = 0.1 ml/min; T = 130°C
13. Background, absorption, desorption, and cooling using the syringe pump setup; N_2 flow rate = 250 ml/min; H_2O flow rate = 0.2 ml/min; T = 130°C
14. Water/capacitance calibration using the syringe pump setup; N_2 flow rate = 250 ml/min; H_2O flow rate = 0.2 ml/min; T = 130°C

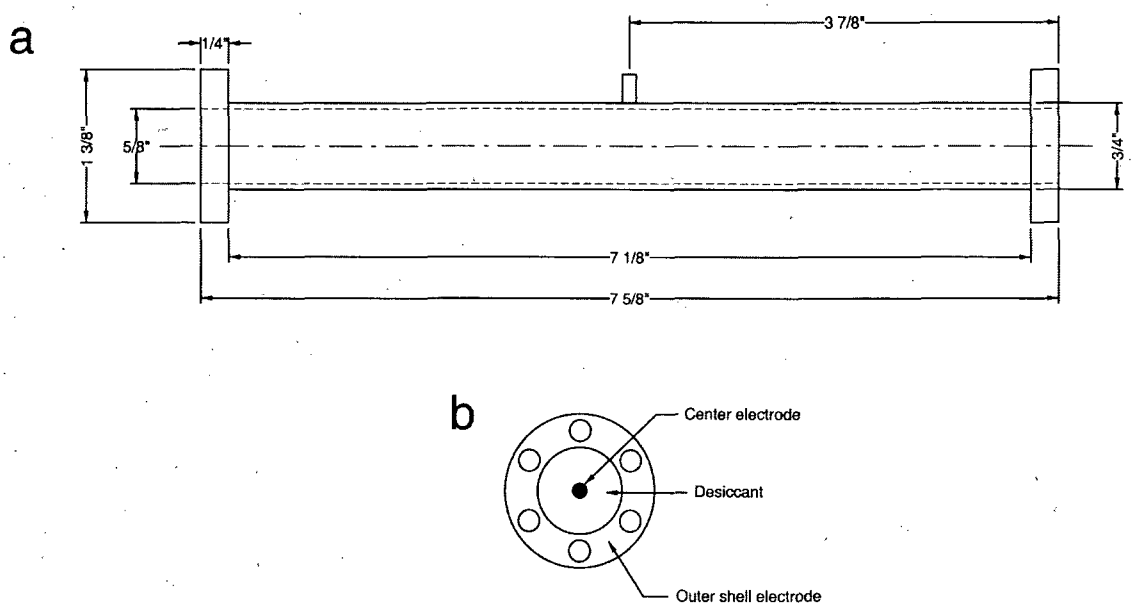

Figure 1: (a) Water desiccant bed without sensor; (b) end-view of bed with sensor

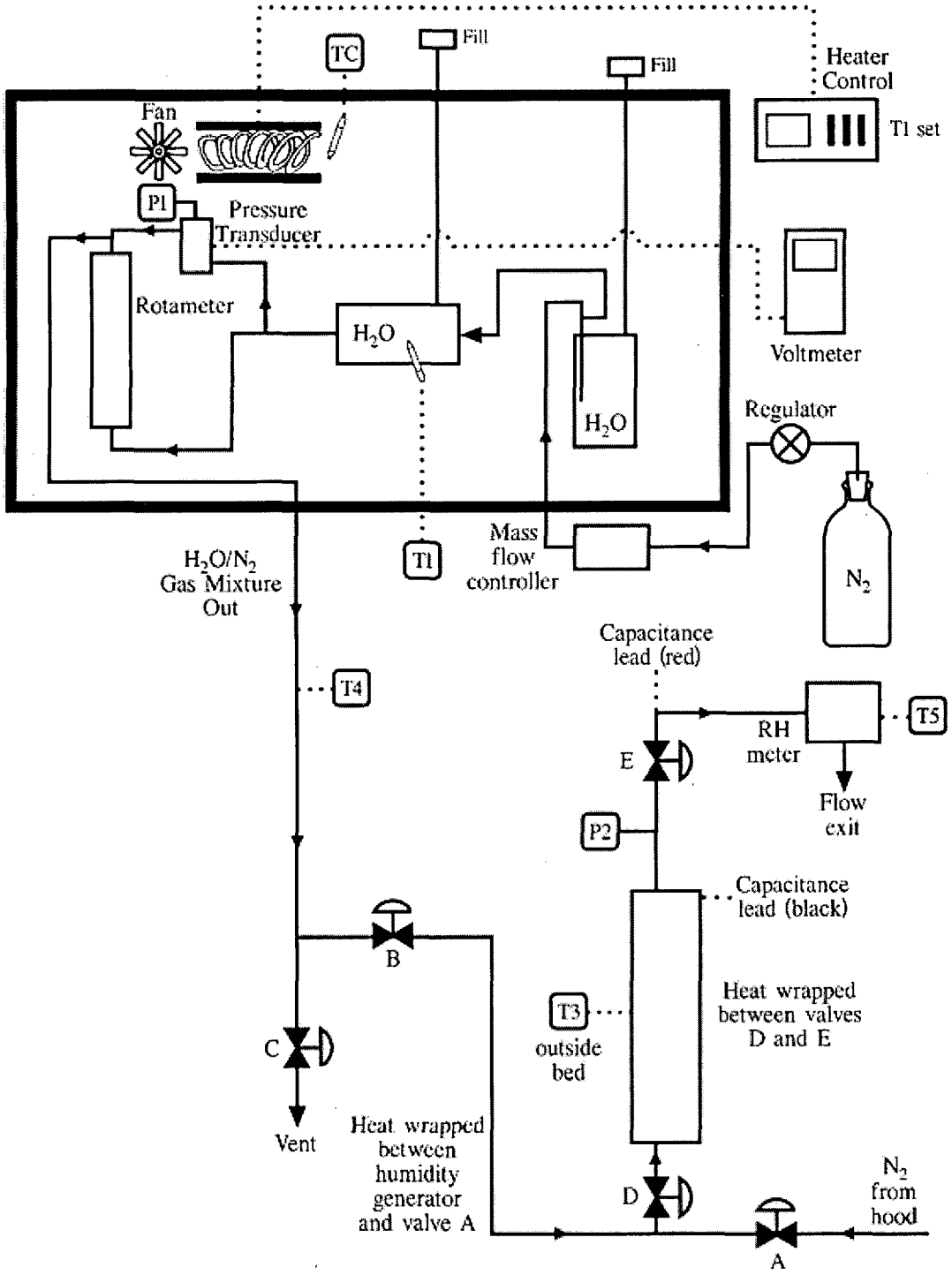

Figure 2: Humidity chamber experimental setup

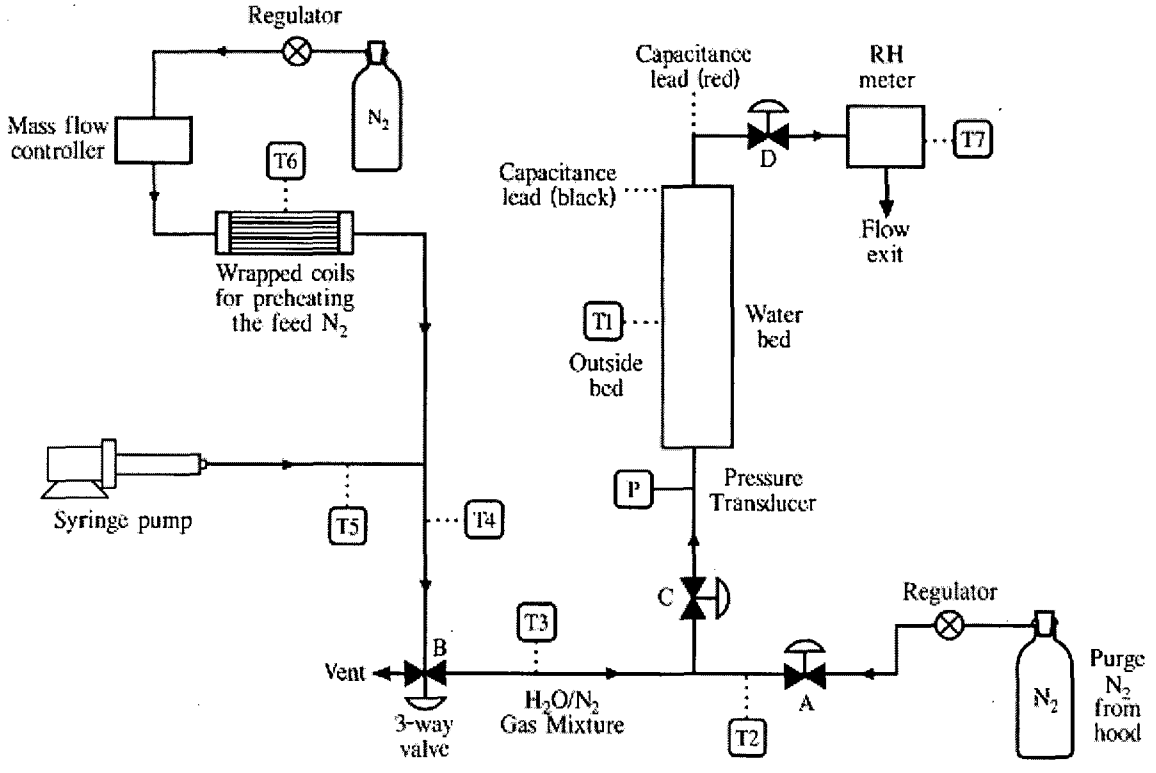

Figure 3: Syringe pump experimental setup

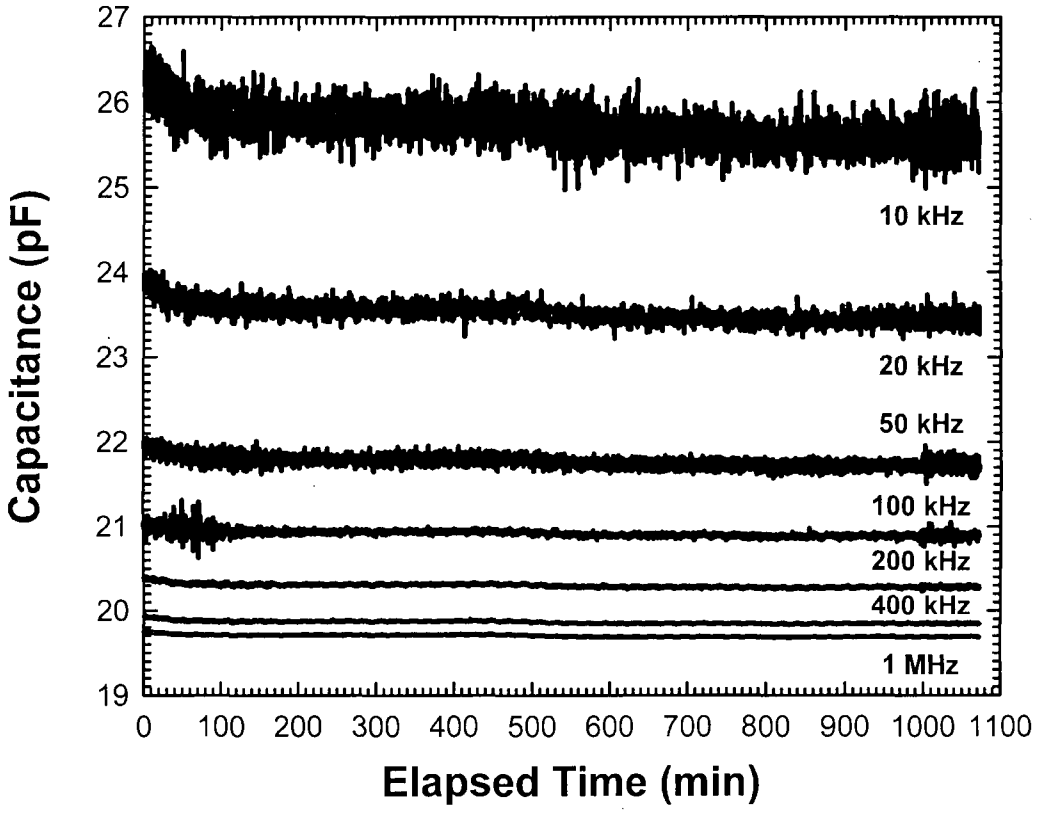

Figure 4: Sealed dry water bed maintained at 130°C overnight

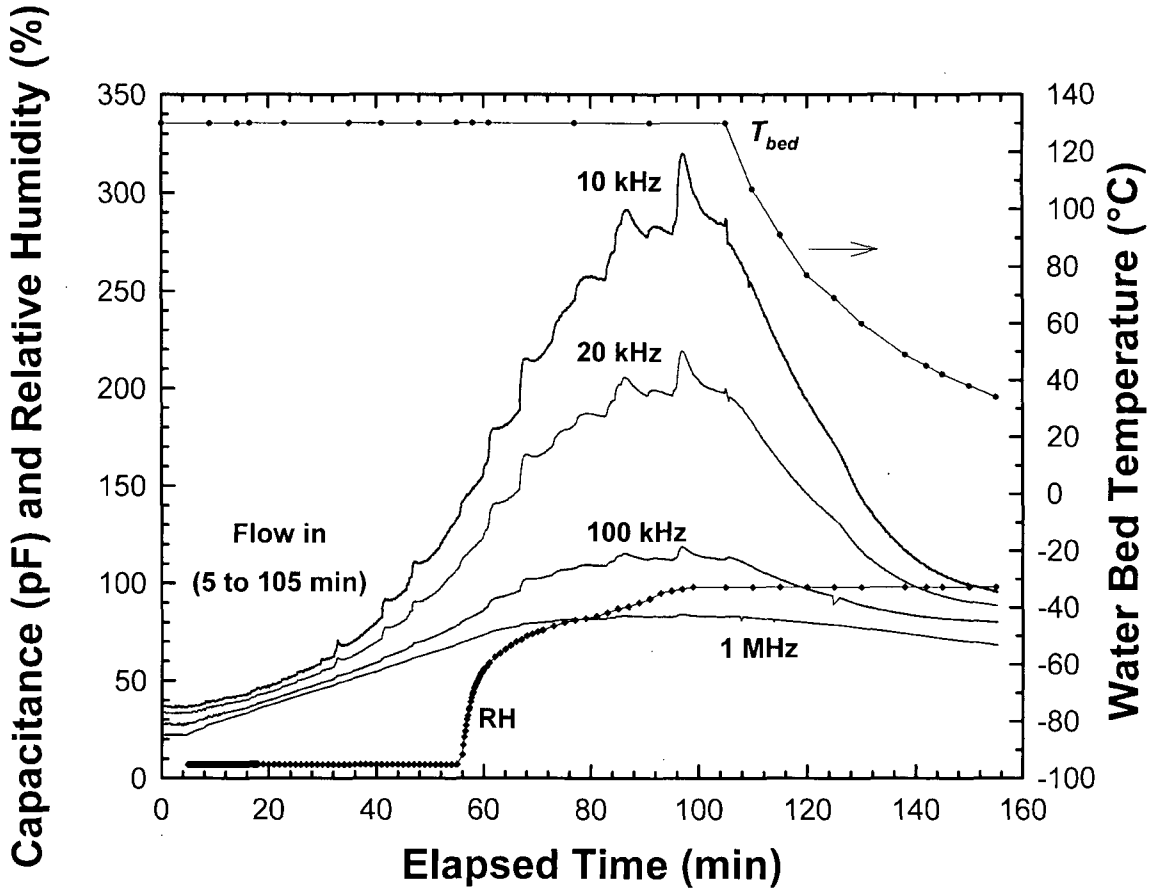

Figure 5: Capacitance, temperature, and relative humidity measurements using the humidity chamber setup; temperature (T_{bed}) refers to the right hand axis; all other plots refer to the left hand axis

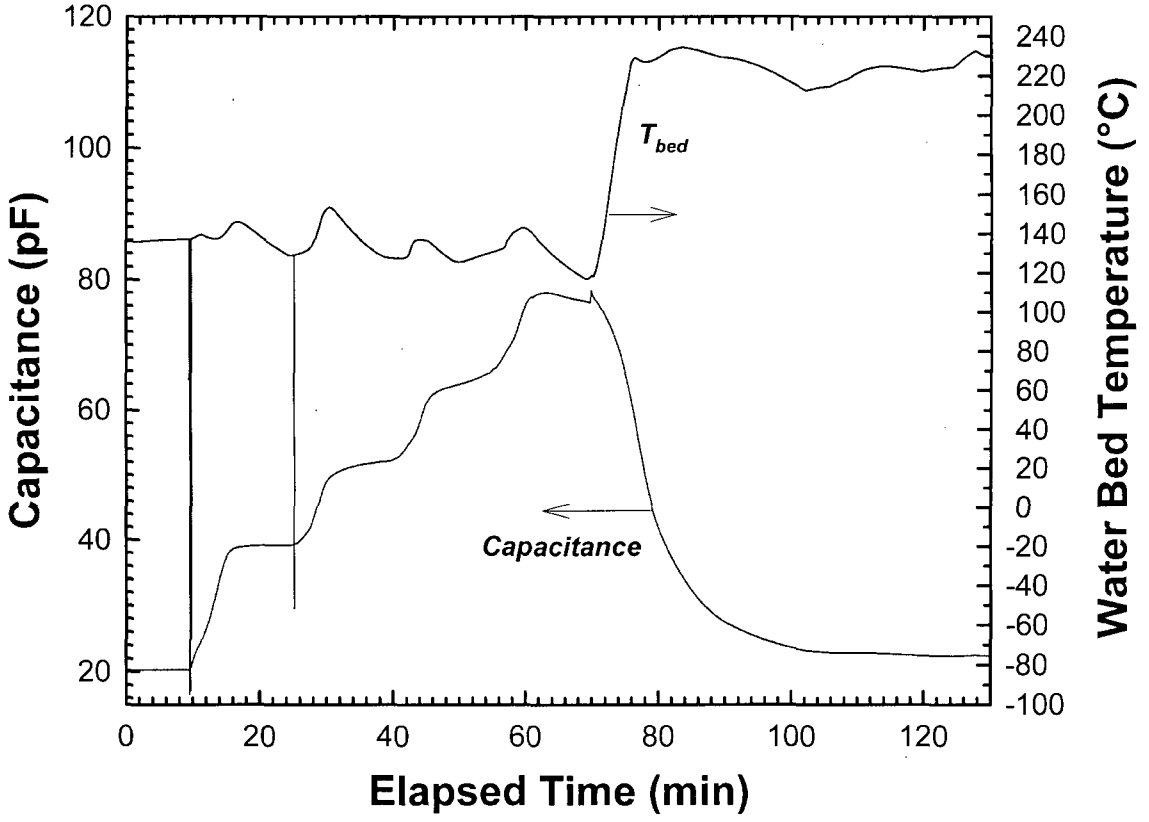

Figure 6: Stepped water experiment using 0.5 g H_2O increments and the syringe pump setup; N_2 flow rate = 250 ml/min; H_2O flow rate = 0.1 ml/min; f = 1 MHz; T = 130°C

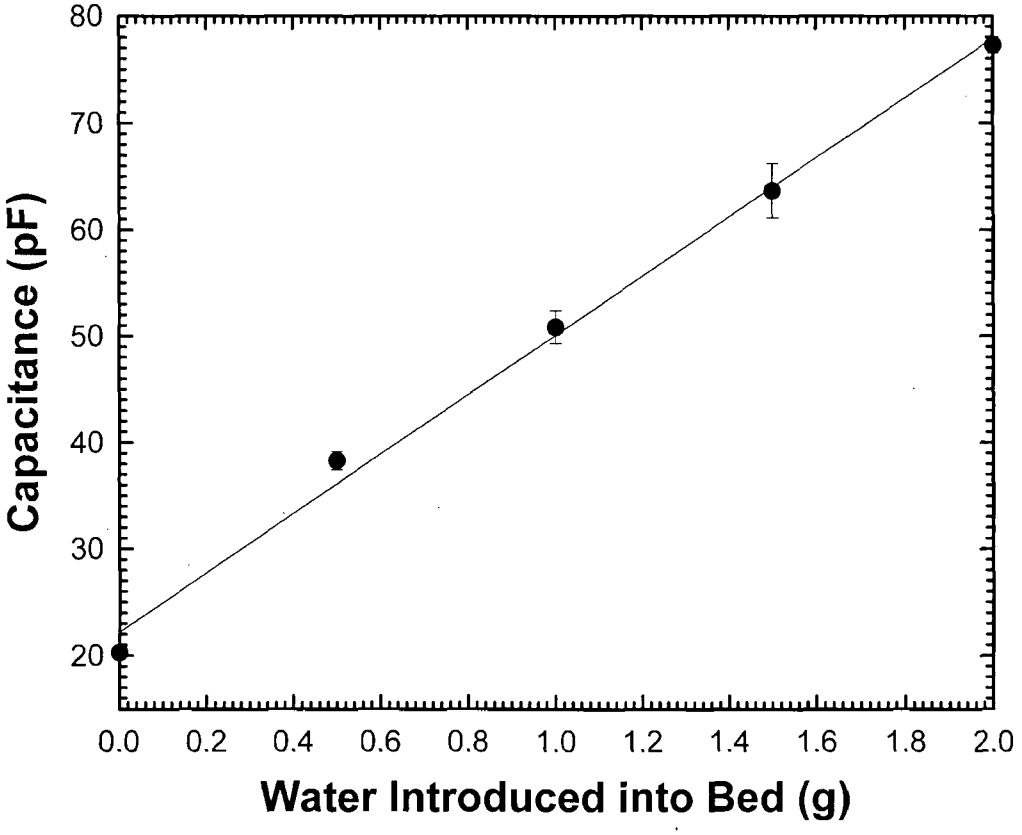

Figure 7: Plateau capacitance values; error bars indicate the extremes in the capacitance at a given step; syringe pump setup; N_2 flow rate = 250 ml/min; H_2O flow rate = 0.1 ml/min; f = 1 MHz; T = 130°C; regression: $C = 27.87\,[H_2O] + 22.192$; $r^2 = 0.995$

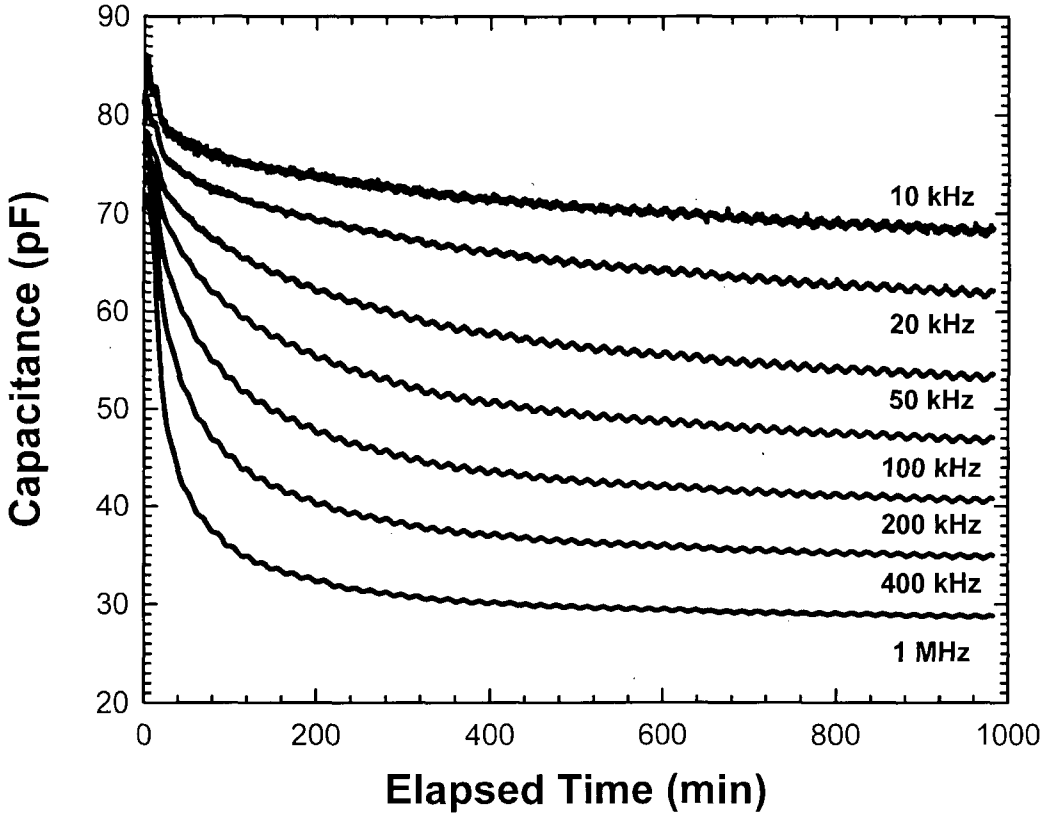

Figure 8: Desorption at 230°C overnight

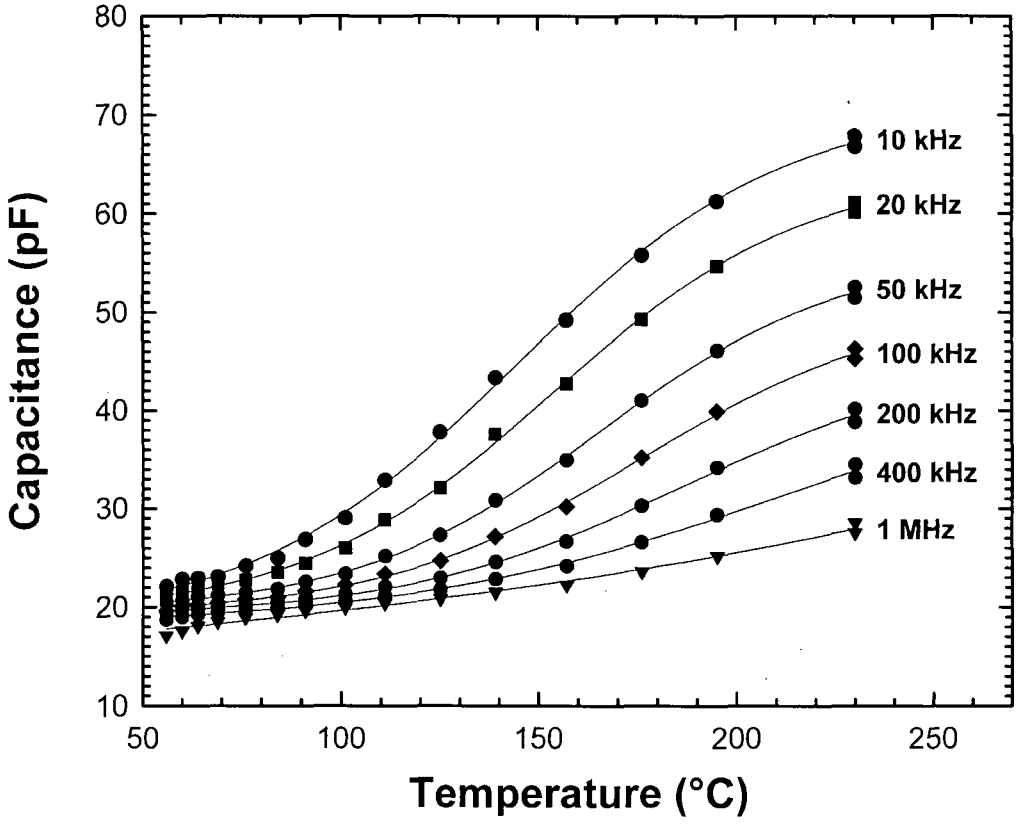

Figure 9: Cooling a dry water bed; data points were fit by 4 parameter sigmoidal regressions

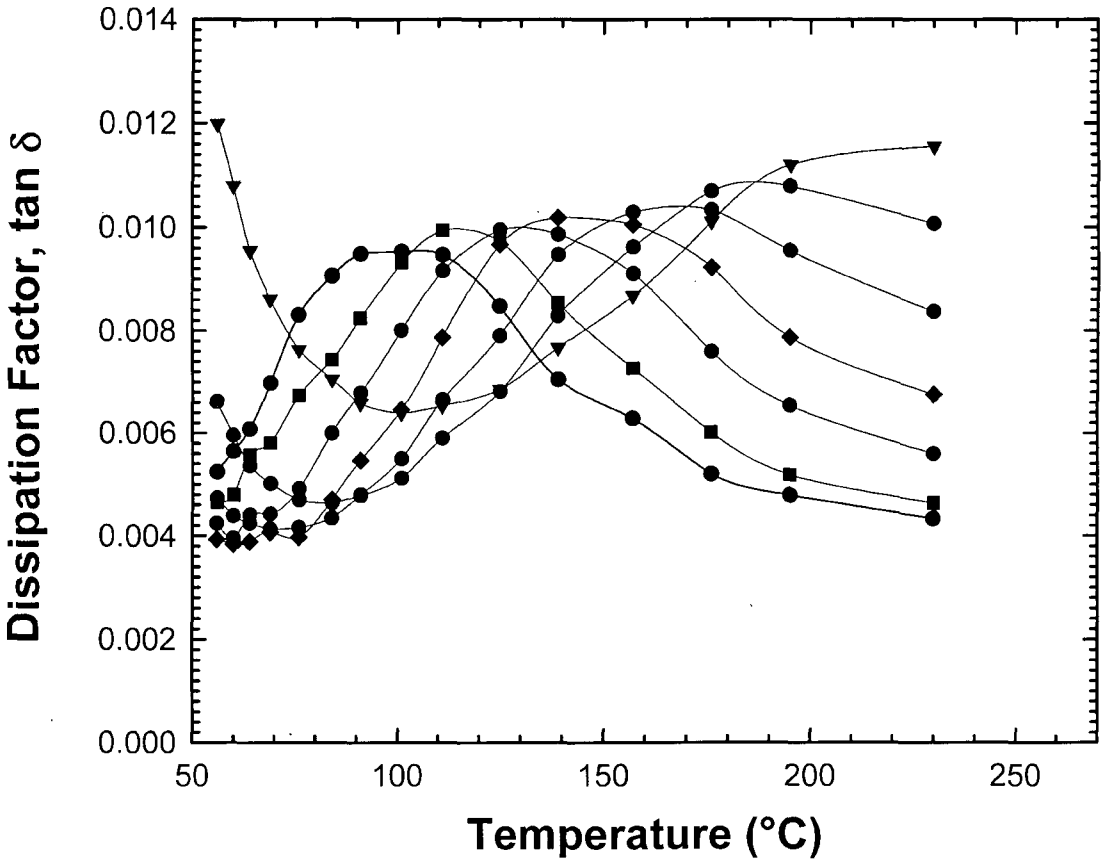

Figure 10: Dissipation factor peaks during cooling after desorption of a dry water bed

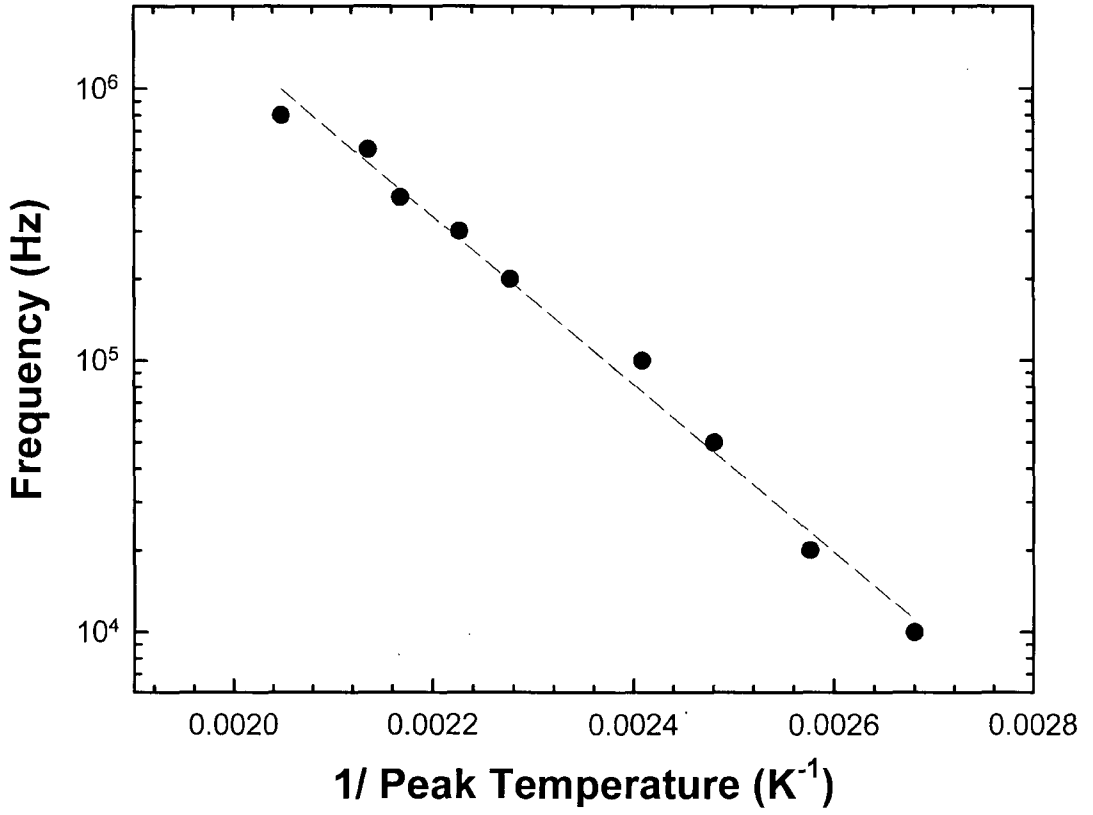

Figure 11: Arrhenius plot of the dry Moisture Gone during cooling after desorption; E_a = 14.15 kcal/mol, r^2 = 0.9904

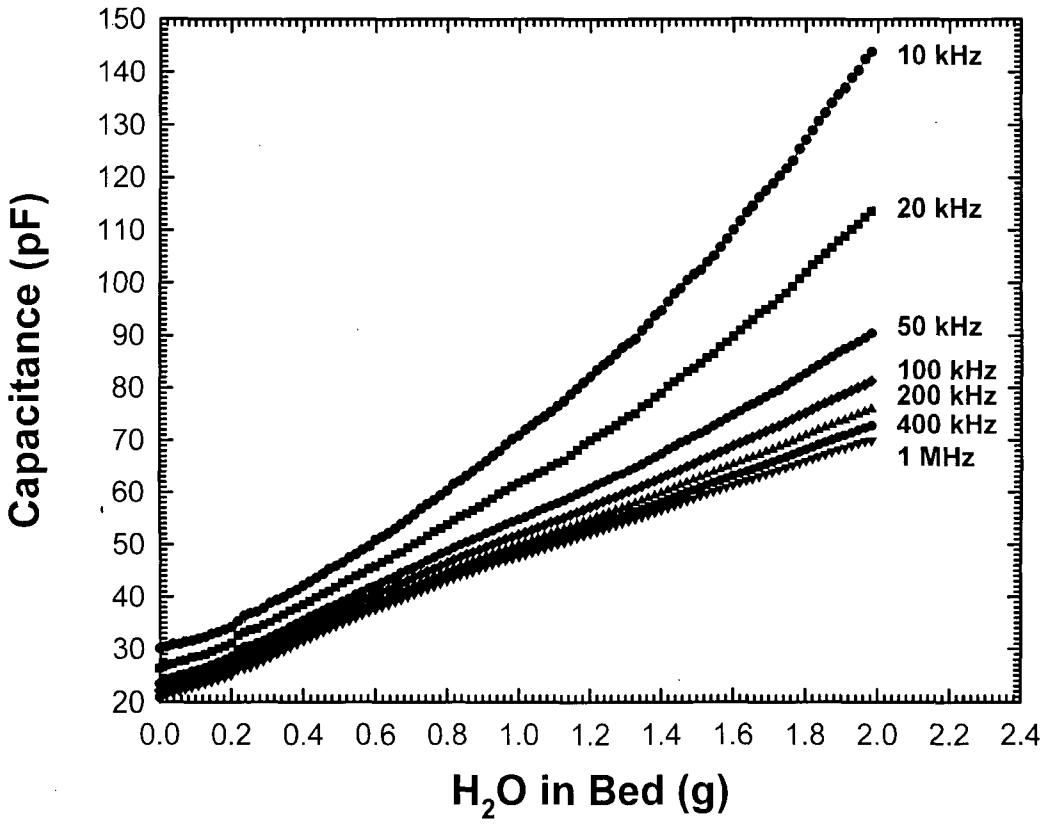

Figure 12: Water/capacitance calibration using the syringe pump setup; N_2 flow rate = 250 ml/min; H_2O flow rate = 0.1 ml/min; T = 130°C

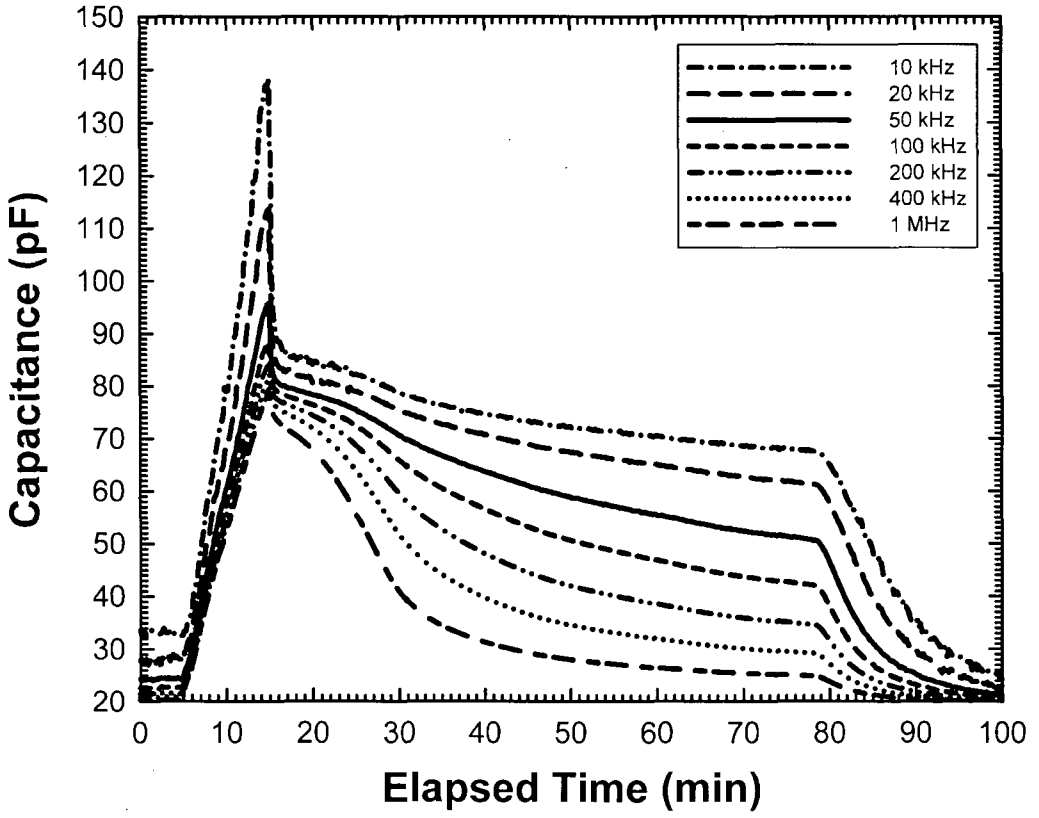

Figure 13: Background, absorption, desorption, and cooling using the syringe pump setup; N_2 flow rate = 250 ml/min; H_2O flow rate = 0.2 ml/min; T = 130°C

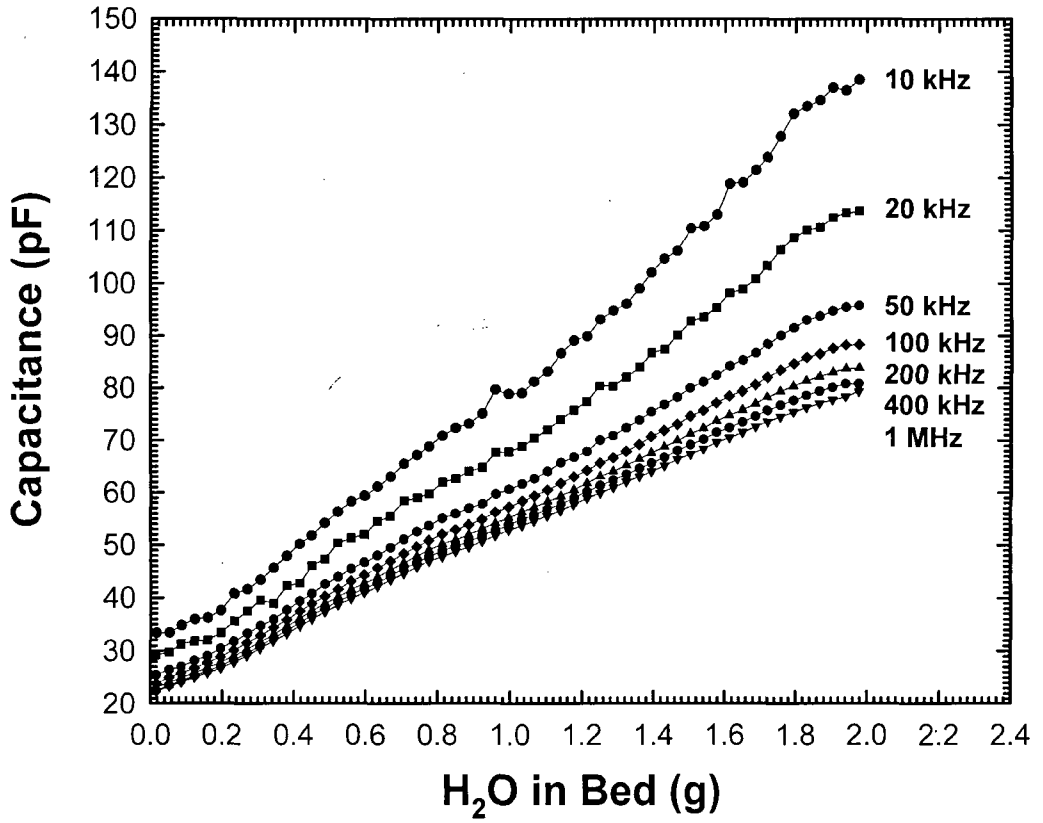

Figure 14: Water/capacitance calibration using the syringe pump setup; N_2 flow rate = 250 ml/min; H_2O flow rate = 0.2 ml/min; T = 130